

POLYMER RHEOLOGY AT HIGH SHEAR RATE FOR MICROINJECTION MOULDING

C. Mnekbi*, M. Vincent, J.F. Agassant

Mines ParisTech – Centre de Mise en Forme des Matériaux, CNRS UMR 7635 – Sophia-Antipolis, France

ABSTRACT: In this paper, we present the rheology of a high-density polyethylene for microinjection moulding. At high flow rate, pressure becomes high enough so that shear heating and pressure-dependence of the viscosity cannot be neglected. Moreover, spurt and chaotic defects related to wall slip were encountered. Nevertheless, we used classical data processing. We obtained viscosity at high shear rate which is lower than the viscosity obtained with the Carreau-Yasuda extrapolation of the moderate shear rate data. In order to discuss the origin of this difference, we developed a flow numerical simulation in the capillary where we take into account pressure and temperature dependent viscosity. The relative importance of these phenomena and their coupling is presented. Then, injection moulding experiments were carried out in a plaque mould. Different moulding parameters were tested. A three dimensional injection moulding numerical simulation, using Rem3D software, was carried out. The quality of the different sets of rheological data is assessed by comparing computed and measured pressure.

KEYWORDS: Microinjection moulding, high shear rate, HDPE, numerical simulation, Rem3D.

1 INTRODUCTION

In microinjection moulding, high velocity combined to small flow gaps lead to different flow behaviour compared to classical injection moulding [1]. One of the questions is the viscosity data at high shear rate [2,3], as numerical simulation of mould filling requires precise rheological data. The aim of this work is to identify what physics is involved in such conditions, to obtain viscous rheological data, and to test them by comparing the results of numerical simulation to measurements in an instrumented mould.

2 HDPE RHEOLOGY

2.1 RHEOLOGY EXPERIMENTS

2.1.1 Material

A commercial semi-crystalline thermoplastic, HDPE (high-density polyethylene) with the grade ELTEX HD 6070, is supplied by Ineos. As the HDPE was not stabilised by the supplier, we added 0.1% of a stabilizer (IRGANOX).

2.1.2 Experimental protocol

A rotational rheometer (ARES) is used in dynamic oscillatory mode to determine polymer linear viscoelastic properties at imposed strain. Measurements are performed in a frequency sweep mode (0.1 to 100 rad/s), at an imposed strain of 10 %, for temperatures between 140 and 190 °C. The viscosity, the elastic modulus G' and the viscous modulus G'' are determined.

Then according to the time-temperature superposition principle, the experimental results are superposed on a master curve at a reference temperature, by means of a shift factor a_T .

A capillary rheometer, the Rheoplast, has a conical Couette plastication zone, in which the polymer is melted by shear-heating and by conduction, then relaxed to homogenize the temperature and finally extruded into a capillary. A pressure transducer is mounted immediately above the capillary to record the pressure drop.

The capillary rheometer is used with six dies with diameter D equal to 1 mm and 0.5 mm, and length over diameter L/D ratio equal to 4, 8 and 16 respectively, at 190°C, for injection volume flow rates between 2 and 1018 mm³.s⁻¹. The maximum recorded pressure is 60 MPa.

2.1.3 Flow hypothesis

We suppose a certain number of assumptions for the evaluation of capillary data:

- flow is incompressible, isothermal and established;
- melt sticks to the wall;
- viscosity is not pressure dependent.

These assumptions permit to use Bagley and Rabinowitsch corrections.

2.1.4 Experimental results

First, we selected the large diameter 1mm. We limited apparent shear rate value to a maximum of 10⁴ s⁻¹. We

did not observe extrusion defects. In those conditions the assumptions set out above are true and classical Bagley and Rabinowitsch corrections can be used [4].

Time-temperature superposition was done according to a shift factor to a reference temperature of 190°C.

The viscosity versus the frequency given by the ARES and the viscosity versus the shear rate given by the Rheoplast are shown in Figure 1. We can see that the Cox-Merz transformation is satisfied.

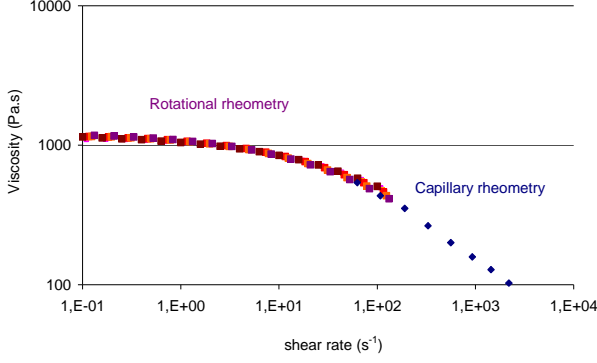


Figure 1: Rotational and capillary rheometries results superimposed for HDPE AT 190°C

In a second step, we imposed high injection speed in the capillary rheometer using the 0.5 mm die diameter. We reach high shear rates values up to 10^5 s^{-1} .

Around a shear rate value of 10^4 s^{-1} , we observe polymer spurt, then chaotic defects. However, the evolution of measured pressure for a constant shear rate still gives a plateau, which permits the determination of a flow curve. HDPE measurements for high shear rate leads to high pressure values up to 60 MPa.

At such a pressure level, dissipative heating and pressure dependent viscosity are no longer negligible [5]. Dissipative heating decreases the viscosity, whereas the rise of pressure enhances the viscosity. Both of these dependencies are estimated afterwards in this paper. We also choose to neglect the extrusion defects for data processing. We employ Bagley and Rabinowitsch corrections to draw viscosity behaviour.

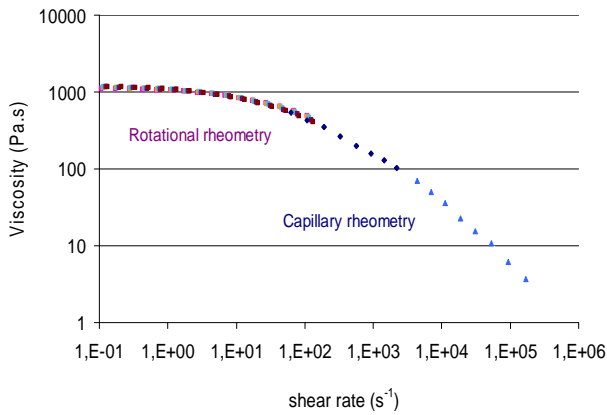


Figure 2: Rotational and high shear rate capillary rheometries results superimposed for HDPE AT 190°C

An extended viscosity curve given by the capillary rheometry is superimposed on the results of Figure 1. The shear rate reaches 10^5 s^{-1} (Figure 2). The viscosity at high shear rate is lower than the viscosity with the Carreau-Yasuda extrapolation of the moderate shear rate data.

2.2 CAPILLARY FLOW SIMULATION WITH TEMPERATURE AND PRESSURE DEPENDENCE OF VISCOSITY

2.2.1 Theoretical issues

At high shear rate, the dissipative heating and pressure dependence of viscosity have to be taken into account [6]. A capillary flow simulation take into account the dissipative and pressure dependent viscosity effect on the pressure.

The viscosity function is expressed by a Carreau-Yasuda law (equation 1).

$$\eta(\dot{\gamma}) = \eta_0 \left[1 + (\lambda \dot{\gamma})^a \right]^{\frac{m-1}{a}} \quad (1)$$

η_0 is zero shear rate viscosity (at T_0 reference temperature and P_0 atmospheric pressure), λ is a characteristic time, m is the power law exponent and a transition width parameter.

The temperature shift factor follows Arrhenius law, (equation 2), as we work with a semi-crystalline thermoplastic:

$$a_T = \exp \left[\frac{Ea}{R} \left(\frac{1}{T} - \frac{1}{T_0} \right) \right] \quad (2)$$

Ea is the activation energy.

Shear rate and temperature dependent viscosity is calculated according to equation 3.

$$\eta(\dot{\gamma}, T) = a_T \eta(\dot{\gamma} a_T, T_0) \quad (3)$$

Shear rate and pressure dependent viscosity (equation 4)

$$\eta(\dot{\gamma}, P) = \exp(\chi P) \eta(\exp(\chi P) \cdot \dot{\gamma}) \quad (4)$$

We can combine both the pressure and temperature dependency of viscosity (equation 5).

$$\eta(\dot{\gamma}, T, P) = \exp(\chi P) \cdot a_T \eta(\exp(\chi P) \cdot \dot{\gamma} a_T, T_0) \quad (5)$$

We assume that the velocity vector is parallel to the tube axis, and the component parallel of the axis z , w , is only a function of the radius r . We assume a generalized Newtonian behaviour law. Neglecting gravity and inertia, the force balance equation leads to:

$$w(r) = \left[\int_R^r \frac{r}{2\eta} dr \right] \frac{dp}{dz} \quad (6)$$

The integration of the flow velocity leads to volume flow rate Q :

$$Q = 2\pi \int_0^R w(r) r dr = 2\pi \frac{dp}{dz} \int_0^R \left(\int_R^r \frac{r}{2\eta} dr \right) r dr \quad (7)$$

We use a slab method to define a bi-dimensional meshing of the capillary. The pressure variation in slab n of length Δz is given by:

$$\Delta P_n = \Delta z \frac{Q}{2\pi \int_0^R \left(\int_0^r \frac{rdr}{2\eta(T_{n-1}, P_{n-1}, \dot{\gamma}_{n-1})} \right) r dr} \quad (8)$$

To determine the temperature regime in the capillary, we calculate the Cameron number for the dissipative heating characterisation. In our case, $Ca \leq 10^{-2}$, the temperature regime is adiabatic.

Dissipative heating for an adiabatic temperature regime in a slab is expressed by (9).

$$\Delta T_n = \frac{\Delta P_n}{\rho \cdot c} \quad (9)$$

Where ρ is the density and c is the specific heat capacity. The simulation is run with a power law initialisation in the first slab. Then, we calculate ΔP_i and ΔT_i in each slab i successively. At the end of calculi, we deduce the P_i values.

2.2.2 Modelling results

We simulate the HDPE flow into a die with a ratio L/D of 8 at 200°C . The geometry of the slab method simulation is given by Figure 3. The material parameters are listed in Table 1.

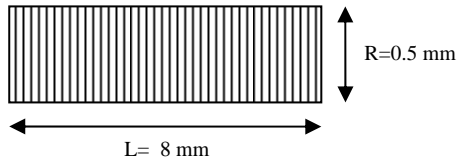


Figure 3: Slab method simulation geometry

We study four cases of flow simulation:
- $\eta(\dot{\gamma})$; $\eta(\dot{\gamma}, T)$; $\eta(\dot{\gamma}, p)$ and $\eta(\dot{\gamma}, T, p)$.

Figure 4 shows the four curves of pressure profile for an imposed shear rate of 10^5 s^{-1} .

Table 1: HDPE parameters at 190°C

Zero shear viscosity	η_0 [Pa.s]	1200
Zero characteristic time	λ [s]	0.01
Transition width parameter	a	1
Power law exponent	m	0.27
Piezodependency coefficient	χ [Pa $^{-1}$]	$2 \cdot 10^{-8}$
Heat capacity	$\rho \cdot c$ [J/ $^\circ\text{Cm}^3$]	$2 \cdot 10^{-6}$
Activation energy	E_a [kJ/mole]	20

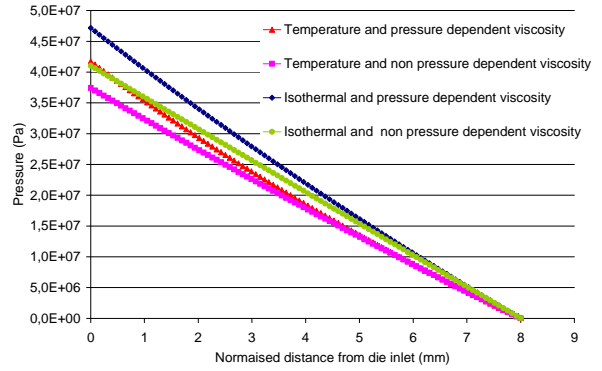


Figure 4: Capillary flow simulation for HDPE at 190°C , shear rate 10^5 s^{-1}

As predicted with experimental observations, the viscosity pressure dependency increases the pressure value in the die, while the dissipative heating decreases this pressure value. But when we combine both the pressure and temperature dependency of viscosity, we return to a pressure value at the die inlet which is the same as the pressure value when both the dependency parameters are not taken into account. As a first approximation of the modelling results, we can suppose that the experimental results at high shear rate are still valid.

3 INJECTION MOULDING

3.1 INJECTION MOULDING EXPERIMENTS

Injection moulding experiments were carried out in a plaque mould 0.5 mm thick, 25 mm long and 25 mm wide, equipped with three pressure sensors P_1 in the channel, P_2 near the entrance of the plaque, and P_3 near the end. A temperature sensor T_m was placed in the upper part of the mould. A light-absorption sensor was used to detect the polymer crystallization during the process. P_2 and P_3 transducers also gave temperatures T_2 and T_3 (Figure 5). The screw displacement was also recorded. The mould was mounted on a pneumatic Getelec injection moulding machine.

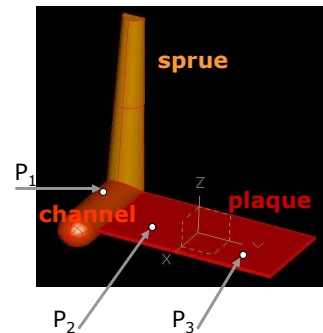


Figure 5: Mould. Only half is represented

Different moulding parameters were tested.

Figure 6 shows the pressures and temperatures recorded during an injection moulding test, with a pneumatic injection pressure of 0.5 MPa . The melt temperature is

240°C and the mould temperature is 75°C. The average shear rate reached 5.10^4 s^{-1} . We can see that the displacement of the screw vs. time is not linear. Therefore, the entrance flow rate is not constant. At the end of mould filling, at 0.29 s, we observe a pressure increase due to the material compressibility.

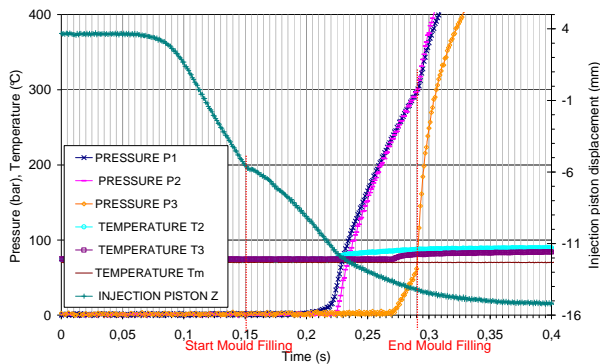


Figure 6: HDPE injection moulding test acquisition

3.2 INJECTION MOULDING SIMULATION

A three dimensional injection moulding numerical simulation, using Rem3D software, was carried out. This simulation was based on finite element equation solvers (a flow Stokes solver, a flow front transport equation solver and a heat equation solver). The entire cavity to be filled was meshed with tetrahedral elements using a fully automatic 3D mesh generator. The finite element method was used to solve the thermo-mechanical equilibrium equations at each time step of the process. We used a thermo dependent Carreau-Yassuda law taking into account the material compressibility. The filled part is shown in Figure 6. The quality of the different sets of rheological data is assessed by comparing computed and measured pressure Figure 7.

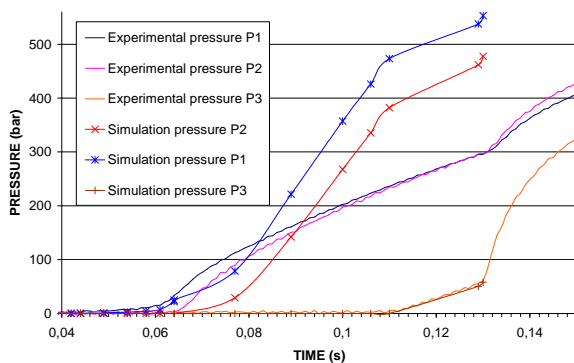


Figure 7: Measured and computed pressures comparisons

The starts of each pressure P1, P2 and P3 are well reproduced by the computation. The filling end coincides in both cases. Nevertheless, the computed pressure values P1 and P2 are more important than the experimental ones. This can be due to the incertitude of the introduced flow rates in the simulation. Another hypothesis for this difference is the material data. We consider a rheology neglecting the wall sleep related to

the extrusion defects and observed in the flow curves. A wall sleep causes a pressure decrease in the measured case.

4 CONCLUSIONS

We presented the rheology of a high-density polyethylene. When we used a capillary rheometer with conventional diameter (1 mm) and injection speed, we obtained viscosity data up to an apparent shear rate of 10^3 s^{-1} . When using smaller diameter (0.5 mm) at high injection rate, the apparent shear rate reached 10^5 s^{-1} . Pressure became high enough so that shear heating and pressure-dependence of the viscosity could not be neglected. Moreover, spurt and chaotic defects related to wall slip were encountered. Nevertheless, we again used classical data processing. We obtained viscosity at high shear rate which is lower than the viscosity obtained with the Carreau-Yasuda extrapolation of the moderate shear rate data. In order to discuss the origin of this difference, we developed a flow numerical simulation in the capillary where we took into account pressure and temperature dependent viscosity. We deduced that at shear rate until 10^5 s^{-1} , the decrease of the pressure due to the heat dissipation and its growth due to the piezodependency cancelled out mutually. In other words, the experimental results at high shear rate should still be valid.

We exploited the experimental rheological data and we tested them by comparing the results of injection moulding numerical simulation to measurements in an instrumented mould. In the simulation, we overestimated the measured pressure.

ACKNOWLEDGEMENT

The authors gratefully acknowledge financial support from the French Research National Agency ANR for Microconnect project. The injection moulding tests were carried out thanks to G. Regnier and N. Bou Malhab from LIM of Ensam Paris.
<http://www.microinjectionmolding.eu/>

REFERENCES

- [1] Whiteside BR, Spares R, Howell K, Martyn MT, Coates PD, Micromolding: extreme process monitoring and inline product assessment, Plastic rubber and composites 34 (9), 2005
- [2] Takahashi H, et al. Rheological behavior of SAN PC blends under extremely high shear rate, Journal of Applied Polymer Science, Vol 37, 1989
- [3] Cardinaels R, et al., Evaluation and comparison of routes to obtain pressure coefficients from high-pressure capillary rheometry data, Rheology Acta, 2007
- [4] Agassant J.-F., Avenas P., Sergent J.-P., Vergnes B., Vincent M. : La mise en forme des matières plastiques, Paris Lavoisier TEC & DOC, 73-74, 1996.
- [5] Couch M. A.; Binding, D. M.; High pressure capillary rheometry of polymeric fluids, Polymer, 2000
- [6] Laun HM, "Capillary rheometry for polymer melts revisited", Rheol acta 43: 509-528, 2004